THE JOURNAL OF BIOLOGICAL CHEMISTRY VOL. 285, NO. 39, pp. 30091–30102, September 24, 2010

Identification of Direct and Indirect Effectors of the Transient Receptor Potential Melastatin 2 (TRPM2) Cation Channel*[S]

Received for publication, September 15, 2009, and in revised form, June 18, 2010 Published, JBC Papers in Press, July 22, 2010, DOI 10.1074/jbc.M109.066464

Balázs Tóth and László Csanády[1]

From the Department of Medical Biochemistry, Semmelweis University, Budapest H-1094, Hungary

Transient receptor potential melastatin 2 (TRPM2) is a Ca^{2+}-permeable cation channel involved in physiological and pathophysiological processes linked to oxidative stress. TRPM2 channels are co-activated by intracellular Ca^{2+} and ADP-ribose (ADPR) but also modulated in intact cells by several additional factors. Superfusion of TRPM2-expressing cells with H_2O_2 or intracellular dialysis of cyclic ADPR (cADPR) or nicotinic acid adenine dinucleotide phosphate (NAADP) activates, whereas dialysis of AMP inhibits, TRPM2 whole-cell currents. Additionally, H_2O_2, cADPR, and NAADP enhance ADPR sensitivity of TRPM2 currents in intact cells. Because in whole-cell recordings the entire cellular machinery for nucleotide and Ca^{2+} homeostasis is intact, modulators might affect TRPM2 activity either directly, by binding to TRPM2, or indirectly, by altering the local concentrations of the primary ligands ADPR and Ca^{2+}. To identify direct modulators of TRPM2, we have studied the effects of H_2O_2, AMP, cADPR, NAADP, and nicotinic acid adenine dinucleotide in inside-out patches from *Xenopus* oocytes expressing human TRPM2, by directly exposing the cytosolic faces of the patches to these compounds. H_2O_2 (1 mM) and enzymatically purified cADPR (10 μM) failed to activate, whereas AMP (200 μM) failed to inhibit TRPM2 currents. NAADP was a partial agonist (maximal efficacy, ~50%), and nicotinic acid adenine dinucleotide was a full agonist, but both had very low affinities ($K_{0.5}$ = 104 and 35 μM). H_2O_2, cADPR, and NAADP did not enhance activation by ADPR. Considering intracellular concentrations of these compounds, none of them are likely to directly affect the TRPM2 channel protein in a physiological context.

TRPM2[2] is a member of the transient receptor potential family of proteins and forms a nonselective cation channel that is permeable to Ca^{2+} (1). TRPM2 channels are abundantly expressed in the brain, in hematopoietic tissues, and in leukocytes (1–4) and activate under conditions of oxidative stress to cause elevations in intracellular $[Ca^{2+}]$ ($[Ca^{2+}]_i$) that contribute to chemotactic responses (5) and chemokine production (6) of immune cells, as well as to neuronal cell death following ischemia (4, 7, 8).

The primary activators of TRPM2 are ADP-ribose (ADPR) and Ca^{2+} (2–4); simultaneous binding of both agonists is required for channel opening (9). TRPM2 channels are homotetramers (10), and ADPR binds to the NUDT9-H domains located at the cytosolic C termini of the subunits, named based on sequence homology to the mitochondrial enzyme NUDT9 (2). Both NUDT9 and isolated NUDT9-H bind ADPR and convert it to AMP and ribose-5-phosphate (2, 11), but the role in TRPM2 channel gating of the very slow ADPR hydrolase (ADPRase) activity of NUDT9-H is unknown. In intact cells ADPR activates TRPM2 only in the presence of either intra- or extracellular Ca^{2+} (4, 12, 13); biophysical studies in inside-out patches have shown that the activatory Ca^{2+}-binding sites are located intracellularly of the gate, such that extracellular Ca^{2+} needs to permeate through the pore before reaching its binding sites (4, 9). Nevertheless, the vicinity of these sites to the pore suggests that in intact cells extracellular Ca^{2+} is the primary source of this activating ligand (9).

What are the signals that initiate TRPM2 channel activity in a cellular context? Early on TRPM2 currents have been linked to the redox status of the cell (4), and several studies have pinpointed oxidative stress, such as that inducible by H_2O_2, as a causative agent in TRPM2 activation. One early report of H_2O_2-activated whole-cell currents from a truncated TRPM2 construct no longer responsive to ADPR (14) could not be reproduced (15). On the other hand, several mutations and deletions in the conserved Nudix motif (RILRQE) of the NUDT9-H domain that abrogated ADPR binding yielded channels that also failed to activate in response to H_2O_2 (4, 15), leading to the conclusion that H_2O_2 acts indirectly by increasing intracellular [ADPR]. Intriguingly, recent reports of synergistic effects between subthreshold concentrations of ADPR and H_2O_2 and of differential inhibitory profiles of ADPR- and H_2O_2-induced whole-cell TRPM2 currents again raised the possibility that H_2O_2 might directly affect TRPM2 activity by a mechanism independent of ADPR (16, 17).

Several additional compounds, mostly adenine nucleotides, have been found to modulate TRPM2 whole-cell currents in different cell types, but there is also substantial disagreement between the various reports. Cyclic ADPR (cADPR) fully stimulated TRPM2 currents in some studies (17, 18), whereas it had little (16) or no (2, 4, 5) effect in others. In addition, small (subthreshold) concentrations of cADPR resulted in large, up to 100-fold, sensitization toward activation by ADPR (16–18), whereas others have found no such synergy (5). More recently,

* This work was supported by Országos Tudományos Kutatási Alapprogramok (OTKA) Grant F 68143 (to L. C.).

[S] The on-line version of this article (available at http://www.jbc.org) contains supplemental Figs. S1 and S2.

[1] Bolyai Research Fellow of the Hungarian Academy of Sciences. To whom correspondence should be addressed: Semmelweis University, Dept. of Medical Biochemistry, Tűzoltó u. 37–47, Budapest, H-1094, Hungary. Tel.: 36-1-459-1500, Ext. 60048; Fax: 36-1-267-0031; E-mail: laszlo.csanady@eok.sote.hu.

[2] The abbreviations used are: TRPM, transient receptor potential melastatin; ADPR, ADP-ribose; cADPR, cyclic ADPR; NAADP, nicotinic acid adenine dinucleotide phosphate; NAAD, nicotinic acid adenine dinucleotide.

nicotinic acid adenine dinucleotide phosphate (NAADP) was reported to fully activate endogenous TRPM2 currents in Jurkat T-lymphocytes (18) and neutrophil granulocytes (17) and to potentiate ADPR-mediated channel activation just as reported for cADPR (17, 18). Finally, ADPR-activated whole-cell TRPM2 currents are inhibited by intracellular dialysis of AMP but are not sensitive to the cADPR analog 8-Br-cADPR (16). In contrast, at least some fraction of cADPR-, NAADP-, and H_2O_2-induced currents seems AMP-resistant but sensitive to inhibition by 8-Br-cADPR (16–18). Low affinity activation of TRPM2 currents by NAD (3, 4) is likely due to contamination by ADPR (16, 19), and the significance of TRPM2 activation by *O*-acetylated ADPR remains to be elucidated (19).

Although the above whole cell patch-clamp studies have identified several interesting compounds as candidates that might directly affect TRPM2 channels, the conclusions of these reports are limited by the fact that in whole-cell recordings the entire cellular machinery involved in nucleotide and Ca^{2+} homeostasis is in place. Thus, intracellular dialysis of a compound might affect TRPM2 activity either directly, by binding to the TRPM2 protein, or indirectly, by altering the local concentrations of the primary ligands ADPR and Ca^{2+}; possible perturbations of other signaling pathways that ultimately affect TRPM2 activity also have to be considered. Regulation of cytosolic [ADPR] is the result of a complex interplay between several cytosolic, nuclear, and mitochondrial enzymes that produce and break down ADPR or that are involved in its translocation between compartments (reviewed in Refs. 20 and 21). It is likely that intracellular dialysis of high concentrations of adenine nucleotides, which are substrates and/or products of several of these enzymes, will ultimately affect cytosolic [ADPR]; just as a bulk overload of intact cells with Ca^{2+} is likely to cause generation of reactive oxygen species and consequent ADPR production, as suggested by gradual activation of whole-cell TRPM2 currents under such conditions (22). Likewise, intracellular [Ca^{2+}] is dynamically regulated by Ca^{2+} release from intracellular stores and plasma membrane Ca^{2+} influx, counteracted by transporters that extrude Ca^{2+} from the cytosol. Acting on ryanodine receptors and on a distinct class of receptors, respectively, both cADPR and NAADP are potent Ca^{2+} mobilizing agents (reviewed in Refs. 23 and 24), which likely alter both bulk intracellular [Ca^{2+}] and its microdomains when dialyzed into cells. Therefore, from whole-cell experiments a direct action of these compounds on the TRPM2 protein cannot be concluded.

To differentiate between direct and indirect effects on TRPM2, we have evaluated these compounds in cell-free inside-out patches using direct ligand superfusion. Our results indicate that H_2O_2, AMP, and cADPR in their pure forms do not directly affect TRPM2 gating. NAADP is a partial and nicotinic acid adenine dinucleotide (NAAD) a full agonist, both capable of directly activating TRPM2, but based on their low apparent affinities it seems unlikely that they should act as direct modulators of TRPM2 currents *in vivo*. These results single out the primary ligands ADPR and Ca^{2+} as the final common pathway into which multiple metabolic routes converge to modulate TRPM2 activity in intact cells.

EXPERIMENTAL PROCEDURES

Molecular Biology— hTRPM2/pGEMHE was constructed as described (9). For *in vitro* transcription plasmid DNA was linearized by NheI; cRNA was prepared using a T7 mMessage mMachine kit (Ambion) and quantified on denaturing gels.

Isolation and Injection of Xenopus Oocytes—*Xenopus* oocytes were isolated and injected with cRNA as previously described (9). Isolated oocytes were stored at 18 °C in a Ringer's solution supplemented with 1.8 mM $CaCl_2$ and 50 μg/ml gentamycin. Macroscopic current recordings were obtained 2–3 days after injection of 10 ng of hTRPM2 cRNA.

Excised Patch Recordings—Inside-out patch recordings were done at 25 °C in a symmetrical sodium gluconate-based solution at a pipette holding potential of +20 mV (V_m = −20 mV) as described (9). Briefly, the tip of the patch pipette (to ~1-cm height) contained 140 mM sodium gluconate, 2 mM magnesium gluconate$_2$, 10 mM HEPES, pH 7.4, with NaOH. The pipette electrode was placed into a 140 mM NaCl-based solution carefully layered on top to avoid mixing. Bath solution contained 140 mM sodium gluconate, 2 mM magnesium gluconate$_2$, 10 mM HEPES, and either 1 mM EGTA (to obtain zero (~8 nM) Ca^{2+}) or 1 mM EGTA + 760 μM calcium gluconate$_2$ (to obtain 1 μM free [Ca^{2+}]), or 0.1–1 mM calcium gluconate$_2$ (to obtain 15–125 μM free [Ca^{2+}]); pH was adjusted to 7.1 with NaOH. Na_2-ADPR, cADPR, Na_2-NAADP, sodium NAAD, and Na_2-AMP (Sigma) were added from aqueous stock solutions. Bovine calmodulin (Calbiochem) was added from a 400 μM stock solution. To compensate for Ca^{2+} binding by the protein and EDTA content of this preparation, 2 μM calmodulin was supplemented with 25 μM calcium gluconate$_2$; fluorescent measurements using Ca-Green 5N (9) confirmed that free [Ca^{2+}] remained unchanged using this protocol. The continuously flowing bath solution was exchanged using computer-driven electronic valves (HEKA); solution exchange was complete within <1 s. Membrane currents were amplified, filtered at 2 kHz (Axopatch-200B), digitized at 10 kHz (Digidata 1440A), and saved to disk (pCLAMP 10; Molecular Devices, Inc.).

Verification of H_2O_2 Activity—A 10 M aqueous H_2O_2 stock solution was stored at +4 °C, and the activity was periodically verified by permanganometry. In brief, 1 ml of 20% (v/v) H_2SO_4 was added to 1 ml of 100-fold diluted H_2O_2 stock solution and titrated with 0.1 N (0.02 M) $KMnO_4$ (factor determined using 0.1 N oxalic acid). No measurable loss of H_2O_2 activity was detected during the time frame of this study.

Data Analysis—To obtain fractional activation by some test concentration of a given nucleotide, quasi-steady macroscopic TRPM2 current in the test segment was normalized to the maximal activity estimated for the same segment. Because after patch excision TRPM2 currents continuously decline (due to a progressive loss of active channels in the patch (9)), the maximal activity used for normalization was obtained by linear interpolation of the activities in the presence of saturating (32 μM) ADPR, obtained in bracketing segments of record in the same patch. For test applications that preceded exposure to 32 μM ADPR, maximal activity for the test segment was estimated by linear extrapolation of the activities obtained subsequently, in the same patch, upon repeated exposures to 32 μM ADPR.

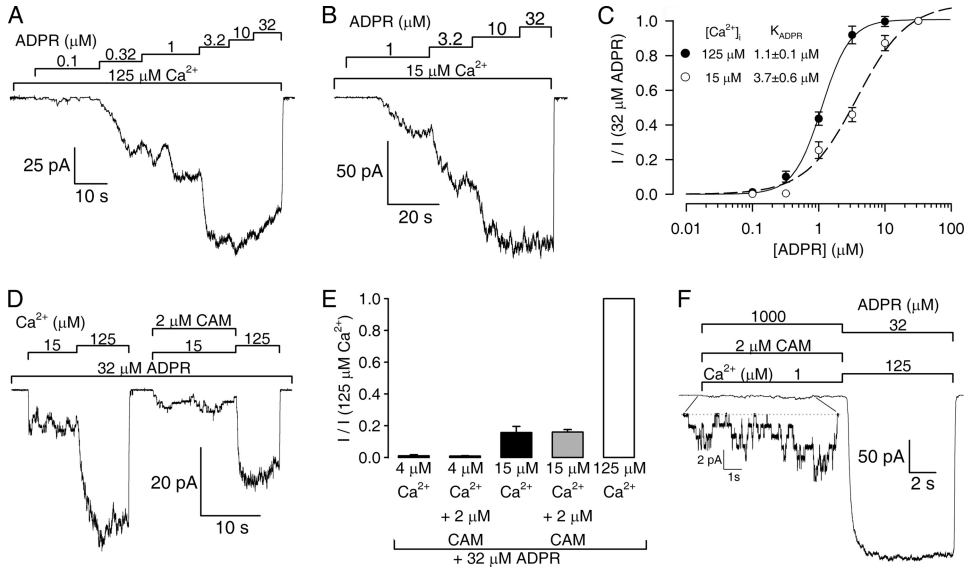

FIGURE 1. **Apparent affinity of TRPM2 for ADPR at saturating and subsaturating $[Ca^{2+}]_i$.** *A* and *B*, inward currents at −20 mV in two inside-out patches excised from *Xenopus* oocytes injected with TRPM2 cRNA, elicited by increasing concentrations of ADPR (*bars*). Intracellular $[Ca^{2+}]$ was 125 μM in *A* and 15 μM in *B*. *C*, normalized dose-response curves for fractional activation by ADPR in the presence of a constant $[Ca^{2+}]_i$ of either 125 μM (*black circles*) or 15 μM (*white circles*). For both curves, the currents were corrected for the rundown (see "Experimental Procedures" and Fig. S1) and normalized to the maximal current obtained in the same patch in the presence of 32 μM ADPR and 125 or 15 μM $[Ca^{2+}]$, respectively. In the case of 125 μM Ca^{2+}, this maximal current corresponds to an open probability of close to unity (9), whereas in 15 μM Ca^{2+} maximal open probability is ~0.2–0.5 (9) (Figs. 1*D*, 2*C*, and 3*E*). The *error bars* represent S.E. *Lines* represent fits to the Hill equation; predicted midpoints are printed in the panel, Hill coefficients were $n_H = 2.0 \pm 0.2$ for 125 μM Ca^{2+} and $n_H = 1.1 \pm 0.2$ for 15 μM Ca^{2+}. *D*, fractional current activation by 15 μM Ca^{2+} in the presence of 32 μM ADPR is not enhanced by the presence of 2 μM calmodulin (*CAM*). *E*, fractional TRPM2 currents activated by 32 μM ADPR in 4 or 15 μM Ca^{2+} in the absence (*black bars*) and presence (*gray bars*) of 2 μM calmodulin. The currents were corrected for rundown as described in supplemental Fig. S1 and normalized to those elicited in the same patch by 32 μM ADPR + 125 μM Ca^{2+} (*white bar*). The *error bars* represent S.E. *F*, in the presence of 1 μM Ca^{2+}, negligible fractional currents are activated even by 1000 μM ADPR co-applied with 2 μM calmodulin (*CAM*); the *inset* shows unitary channel openings in 1 μM Ca^{2+} at an expanded current scale.

This rundown correction protocol is illustrated in supplemental Fig. S1. Dose-response curves were fitted to the Hill equation by nonlinear least squares methods (SigmaPlot 10; SPSS Inc.). The error bars represent S.E.

Enzymatic Purification of cADPR—cADPR was purified from its ADPR contamination using nucleotide pyrophosphatase type I (P7383; Sigma), following a protocol modified from that described in Ref. 5. In brief, 1 unit of the enzyme was added to a 400-μl volume of 2 mM cADPR in the presence of 2 mM $MgCl_2$ and incubated at 37 °C for 60 min. Following incubation the enzyme (molecular mass, ~24 kDa by SDS-PAGE) was removed by 2-fold filtering through 3-kDa molecular mass cut-off filter units (Z629367; Sigma). Analysis of the resulting filtrate by TLC (see below) revealed complete conversion of contaminating ADPR into AMP plus ribose-5-phosphate (see Fig. 5*A*; ribose-5-phosphate shows no fluorescence) but nearly complete recovery of cADPR. At the same time, functional testing confirmed complete removal of the enzyme by the 2-fold filtering procedure (see Fig. 5, *D* and *E*).

Analysis of Nucleotide Purity by Thin Layer Chromatography—Purity of ADPR, cADPR, NAADP, NAAD, and NAD stock solutions was analyzed by blotting 10–100 nmol of nucleotide onto Polygram SIL G/UV_{254} plates (Macherey-Nagel) followed by development in 70% (v/v) ethanol, 30% (v/v) H_2O, 0.2 M NH_4HCO_3 (25). Separated nucleotides were visualized under UV illumination.

RESULTS

Human TRPM2 is efficiently expressed in *Xenopus* oocytes and forms channels with properties similar to those observed in mammalian expression systems (9). In inside-out patches excised from TRPM2-expressing oocytes, macroscopic currents can be routinely obtained. Ligands are applied directly to the cytosolic surface of the membrane; a continuously flowing bath solution affords perfect control over local concentrations of all agonists, whereas the composition of this cytosolic solution is completely exchanged within <1 s. These properties render our system ideal for addressing whether a compound that affects TRPM2 activity in intact cells exerts its effect by directly targeting the TRPM2 protein.

Earlier work has demonstrated that the Ca^{2+}-binding sites responsible for TRPM2 activation are found in a restricted space intracellularly, but in the immediate vicinity of the channel pore, such that the primary source for activating Ca^{2+} is likely extracellular. Even in the face of extremely rapid vectorial rinsing with a buffered zero Ca^{2+} solution, these activating sites experience $[Ca^{2+}]$ in the tens of micromolar range once a channel has opened (9), so this is all the more likely to be true in the static environment of an intact cell, regardless of the bulk $[Ca^{2+}]_i$ achieved using Ca^{2+} buffers. Because only open channels contribute to the measured currents, it follows that during whole-cell experiments the observed currents are due to TRPM2 channels that experience high micromolar $[Ca^{2+}]$ at their activating sites. Thus, in the present study assaying nucleotide-mediated regulation of TRPM2 in inside-out patches under rapid cytosolic perfusion, we used a saturating $[Ca^{2+}]_i$ as our reference condition to achieve a local environment comparable with that experienced by TRPM2 channels in whole-cell studies or in a physiological context (26).

Intracellular $[Ca^{2+}]$ Little Affects Apparent Affinity for Activation of TRPM2 by ADPR—To obtain adequate controls for our experiments testing the effects of various potential modulators both at high and low $[Ca^{2+}]_i$, we first examined to what extent the apparent affinity of the primary ligand ADPR is sensitive to $[Ca^{2+}]_i$. To this end, we assayed macroscopic current responses of patches containing hundreds of TRPM2 channels to increasing concentrations of ADPR while maintaining intracellular free $[Ca^{2+}]$ at a saturating (125 μM) (Fig. 1*A*) or a subsaturating (15 μM; *cf.* $K_{½}$ for Ca^{2+} activation is ~20 μM in saturating [ADPR] (9)) level (Fig. 1*B*). Although the maximally

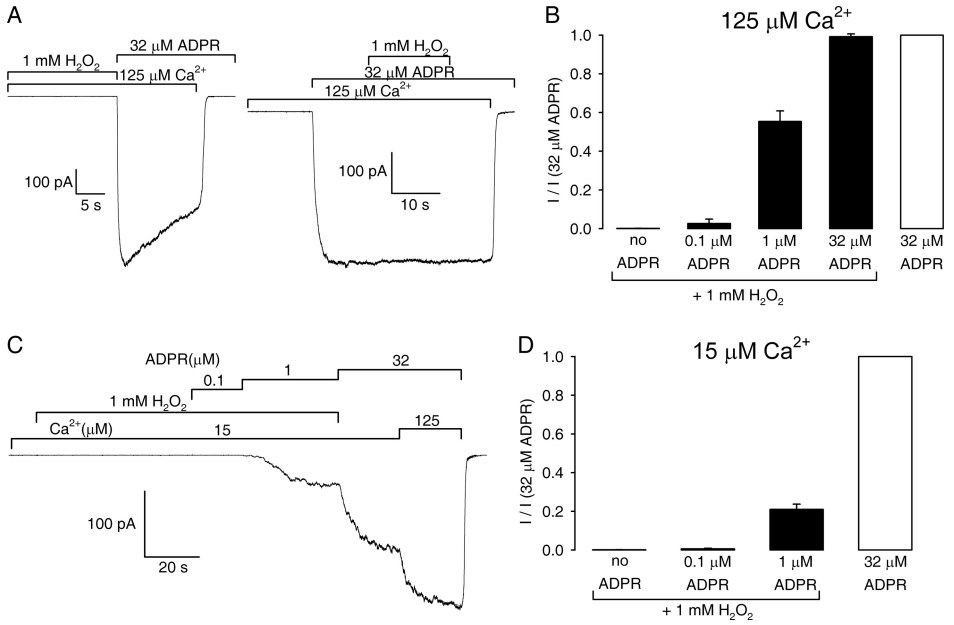

FIGURE 2. **H_2O_2 does not directly affect TRPM2 activity.** *A*, macroscopic current responses of TRPM2 channels in inside-out patches to direct superfusion with H_2O_2. *Left panel*, no current is activated by direct superfusion with 1 mM H_2O_2 in the presence of saturating (125 μM) Ca^{2+} (*bars*), whereas subsequent exposure to 32 μM ADPR elicits a large current indicating ~700 active TRPM2 channels in this patch. *Right panel*, direct superfusion with 1 mM H_2O_2 does not affect TRPM2 currents activated by 32 μM ADPR in the presence of saturating Ca^{2+}. *B*, fractional activation by 0, 0.1, 1, and 32 μM ADPR in the presence of 125 μM Ca^{2+} and 1 mM H_2O_2. Currents in 1 mM H_2O_2 + various concentrations of ADPR (*black bars*) were normalized to those obtained in the same patch by subsequent exposure to 32 μM ADPR (*white bar*). *C*, no current is activated by direct superfusion with 1 mM H_2O_2 in the presence of subsaturating (15 μM) Ca^{2+} (*bars*), and fractional current activation by subsequent exposure to increasing concentrations of ADPR in 15 μM Ca^{2+} is not affected by the maintained presence of 1 mM H_2O_2. *D*, fractional activation by 0, 0.1, and 1 μM ADPR in the presence of 15 μM Ca^{2+} and 1 mM H_2O_2. Currents in 1 mM H_2O_2 + various concentrations of ADPR (*black bars*) were normalized to that obtained in the same patch by subsequent exposure to 32 μM ADPR (*white bar*). The currents were corrected for rundown (see "Experimental Procedures" and Fig. S1); *error bars* in *B* and *D* represent S.E.

activatable current (in 32 μM ADPR) is greatly reduced upon lowering $[Ca^{2+}]_i$ from 125 to 15 μM (Figs. 1*D*, 2*C*, and 3*E* and Ref. 9), the normalized dose-response curve for ADPR activation is only slightly shifted (Fig. 1*C*, *black versus white symbols*); the apparent $K_{½}$ for ADPR, from fits to the Hill equation (Fig. 1*C*, *solid* and *dashed lines*), was 1.1 ± 0.1 μM at 125 μM Ca^{2+} and 3.7 ± 0.6 μM at 15 μM Ca^{2+}.

In Inside-out Patches Calmodulin and Even Millimolar ADPR Fail to Activate TRPM2 Channels at Submicromolar $[Ca^{2+}]$—Because ADPR affinities reported in previous studies were measured in intact cells in which bulk cytosolic Ca^{2+} levels are submicromolar (2, 16, 18), we evaluated the possibility of measuring TRPM2 sensitivity to ADPR at submicromolar Ca^{2+} levels in our cell-free system. In principle, the low affinity of the channels for Ca^{2+} in inside-out patches (9) might be due to the loss of a high affinity Ca^{2+}-binding site upon patch excision. A prime candidate for such a binding site could be calmodulin, which has an intrinsically high Ca^{2+} affinity and has been shown to associate with, and modulate the activity of, TRPM2 (13, 27). However, in the presence of 32 μM ADPR, fractional current activation by low micromolar Ca^{2+} was not affected by superfusion of the cytosolic faces of the patches with 2 μM calmodulin (Fig. 1*D*); a 100-fold lower concentration of biotinylated calmodulin was shown to be sufficient to bind TRPM2 protein in an overlay assay (27). The lack of effect of calmodulin on the apparent Ca^{2+} affinity of TRPM2 in excised patches (Fig. 1*E*, compare *gray versus black bars*) suggests either that calmodulin is not involved in Ca^{2+} activation of TRPM2 or that endogenous calmodulin remains tightly bound to the channels following patch excision.

Because in whole-cell studies apparent Ca^{2+} affinity of TRPM2 was tested at much higher, millimolar, ADPR concentrations (12, 13), we tested whether such a high [ADPR] might eliminate the need for high micromolar cytosolic $[Ca^{2+}]$. Although in the presence of 1 μM Ca^{2+} and 2 μM calmodulin we could indeed observe TRPM2 unitary currents upon exposure to 1 mM ADPR (Fig. 1*F*, *see inset*) (2, 22), subsequent addition of saturating (125 μM) Ca^{2+} revealed that the openings in 1 μM Ca^{2+} reflected a vanishingly low open probability (of ~0.01) of a very large number of channels in the patch. Thus, in excised patches neither calmodulin nor millimolar ADPR alleviates the need for high micromolar Ca^{2+}, suggesting that the activating Ca^{2+}-binding sites on TRPM2 are intrinsically tuned to sense the high local $[Ca^{2+}]$ in the immediate vicinity of the pore (9). For this reason, we were unable to test the effect of various TRPM2 modulators at submicromolar $[Ca^{2+}]$.

H_2O_2 Fails to Activate TRPM2 Channels in a Cell-free System—Whole cell studies conducted in the past have led to contradictory conclusions about the mechanism by which oxidative stress, such as that induced by H_2O_2, leads to TRPM2 activation (4, 14–16). If H_2O_2-mediated activation is independent of ADPR and reflects direct oxidation of some amino acid side chain(s) on the cytosolic surface of the TRPM2 protein, then TRPM2 currents should be activatable in inside-out patches by superfusion with H_2O_2. Because TRPM2 channel opening requires the presence of cytosolic Ca^{2+} (9, 18) (see Figs. 1*D* and 3*A*), we tested whether exposure of inside-out patches to H_2O_2 in the presence of saturating (125 μM) Ca^{2+} is sufficient to activate TRPM2 currents. To this end, patches excised from TRPM2-expressing oocytes were first superfused for various lengths of time with 1 mM H_2O_2 in the presence Ca^{2+} before exposure to a saturating concentration of ADPR (32 μM; see Fig. 1, *A* and *C*) to allow estimation of the number of activatable TRPM2 channels in the same patch (Fig. 2*A*, *left trace*). No TRPM2 channel currents were observed even for incubation times in H_2O_2 lasting longer than 1 min, whereas subsequent exposure to ADPR typically revealed the presence of several hundred activatable TRPM2 channels (Fig. 2*A*, *left trace*; note that because of the typically observed rundown, channel numbers must have been even larger during the periods of exposure

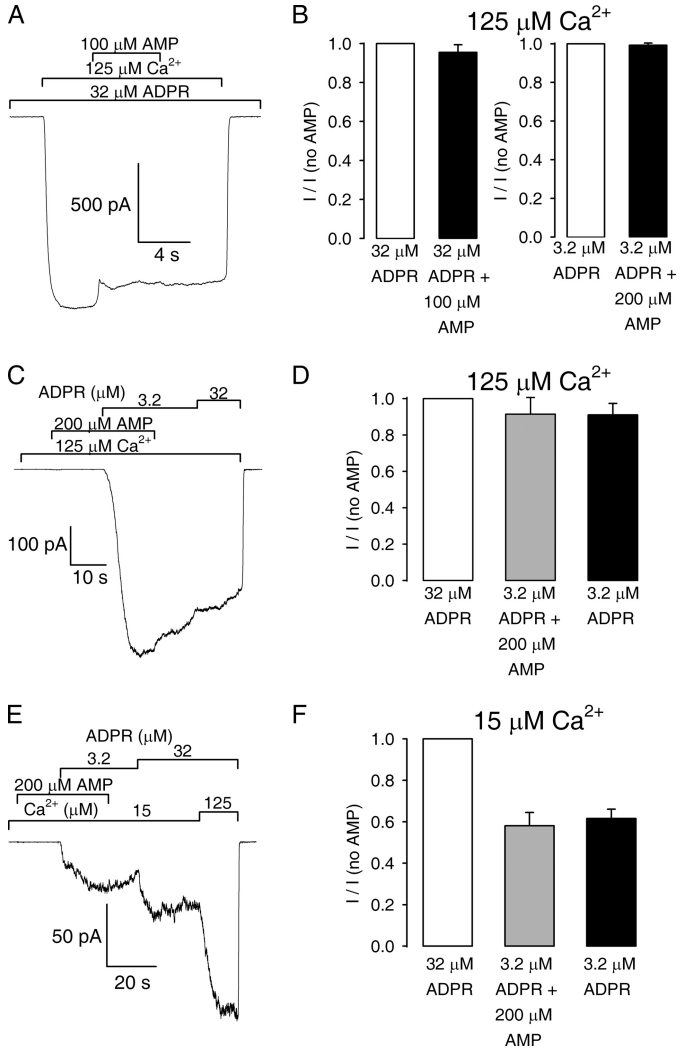

FIGURE 3. **AMP does not inhibit TRPM2 currents in cell-free patches.** *A*, macroscopic TRPM2 current is activated in an inside-out patch by 32 μM ADPR + Ca^{2+} (*bars*); 100 μM AMP is added to test for possible inhibition. *B*, fractional inhibition of ADPR-activated currents by AMP. Currents in the presence of indicated concentrations of AMP + ADPR (*black bars*) were normalized to the average of the currents in bracketing control segments of record obtained in just ADPR (*white bars*). *C* and *E*, pre-exposure to, and maintained presence of, 200 μM AMP does not prevent stimulation of TRPM2 currents by subsequent addition of 3.2 μM ADPR in either saturating (125 μM, *C*) or subsaturating (15 μM, *E*) Ca^{2+}. *D* and *F*, currents elicited in the maintained presence of 200 μM AMP by subsequent addition of 3.2 μM ADPR (*gray bars*) and those obtained in 3.2 μM ADPR following removal of AMP (*black bars*) were normalized to the currents activated by 32 μM ADPR in the same patch (*white bars*); $[Ca^{2+}]_i$ was 125 μM in *D* and 15 μM in *F*. Correction for rundown was done as described for supplemental Fig. S1. The *error bars* in *B*, *D*, and *F* represent S.E.

to H_2O_2). Fractional currents in H_2O_2 from seven similar experiments were not significantly different from zero (Fig. 2*B*, *leftmost bar*). Thus, TRPM2 is not activated by H_2O_2-mediated oxidation of amino acid side chains on the cytosolic surface of the channel. We next tested whether a potential side chain oxidation by H_2O_2 might perhaps inhibit rather than stimulate channel activity. However, the activity of channels that had been opened by 32 μM ADPR was not affected by exposure for up to tens of seconds to 1 mM H_2O_2 (Fig. 2*A*, *right trace*); fractional current remained 0.99 ± 0.01 ($n = 9$) in ADPR + H_2O_2 (Fig. 2*B*, *rightmost black bar*).

We also examined whether H_2O_2 exposure might enhance activation by ADPR, as suggested in recent whole-cell studies (16, 17). However, superfusion of inside-out patches with 0.1 and 1 μM ADPR in the continued presence of 1 mM H_2O_2 activated fractions of 0.026 ± 0.023 ($n = 7$) and 0.55 ± 0.06 ($n = 7$) (Fig. 2*B*, *black bars*), respectively, of maximal current (in 32 μM ADPR), indicating no change in apparent affinity for ADPR in the presence of H_2O_2 ($K_{½} \sim 1$ μM; Fig. 1, *A* and *C*).

Finally, we considered the possibility that the reported facilitatory effect of H_2O_2 might happen through the same or a similar mechanism by which Ca^{2+} potentiates TRPM2 activity. In this case such an effect of H_2O_2 might be masked by our use of a saturating $[Ca^{2+}]_i$. We therefore repeated experiments similar to those summarized in Fig. 2 (*A* and *B*) at a suboptimal $[Ca^{2+}]_i$ of 15 μM (Fig. 2, *C* and *D*). However, just as in saturating $[Ca^{2+}]_i$, exposure to 1 mM H_2O_2 failed to elicit channel openings in 15 μM Ca^{2+} (Fig. 2*C*) and did not affect fractional activation by 0.1 or 1 μM ADPR in 15 μM Ca^{2+} (Fig. 2*D*; compare with Fig. 1*B* and *white symbols* in Fig. 1*C*). Taken together, these results indicate either that no amino acid side chains on the cytosolic face of TRPM2 are oxidized by H_2O_2 or that such oxidation has no functional consequences for TRPM2 channel activity, at least for H_2O_2 concentrations up to 1 mM.

AMP Does Not Affect ADPR-induced TRPM2 Currents in Inside-out Patches—Intracellular perfusion of AMP suppresses ADPR-induced whole-cell TRPM2 currents in a dose-dependent manner (16). Because AMP is one of the cleavage products of the ADPRase reaction reportedly catalyzed by the NUDT9-H domain (2, 11), AMP might inhibit TRPM2 channel activity by competing with ADPR for binding to NUDT9-H. On the other hand, TRPM2 homolog TRPM4 (28) (and native TRPM4-like (29)) cation channels that lack the C-terminal NUDT9-H domain are also inhibited by AMP with high affinity. An alternative possibility therefore is that AMP binds to the large cytosolic N-terminal TRPM homology region present in all TRPM family channels, resulting in noncompetitive inhibition of ADPR-induced TRPM2 activity.

To evaluate these possibilities, we set out to study the kinetics of AMP-mediated inhibition of TRPM2 reported to occur with an IC_{50} of ~70 μM in whole cells (16). To our surprise, TRPM2 currents activated by saturating concentrations of Ca^{2+} and ADPR (125 and 32 μM, respectively) were barely affected by superfusion of the cytosolic face of the channels with 100 μM AMP (Fig. 3*A*), yielding a fractional current of 0.95 ± 0.04 ($n = 6$) in the presence of AMP (Fig. 3*B*, *left panel*, *black bar*). Because in another whole-cell study conducted at a lower [ADPR] AMP inhibited with even higher apparent affinity ($IC_{50} = 10$ μM) (17), we also tested inhibition by AMP at a 10-fold lower [ADPR] (3.2 μM). However, application of AMP concentrations as high as 200 μM failed to affect TRPM2 currents induced by 3.2 μM ADPR, yielding an average fractional current of 0.99 ± 0.01 ($n = 19$) in 200 μM AMP (Fig. 3*B*, *right panel*, *black bar*).

To minimize rundown, in the above experiments (Fig. 3, *A* and *B*) AMP was applied for relatively short time intervals, bracketed by segments of record in AMP-free solution. However, if AMP competes with ADPR for the same binding site, then such brief exposures might not allow AMP to displace

ADPR, because the binding sites have already been preloaded with ADPR at the time of AMP application, and the kinetics of ADPR unbinding might be slow. We therefore tested whether a pre-exposure to AMP might prevent subsequent activation by ADPR (Fig. 3*C*). However, pre-equilibration with 200 μM AMP did not affect subsequent activation (in the continued presence of AMP) by 3.2 μM ADPR (Fig. 3*C*); thus, comparison of current amplitudes (corrected for rundown; see "Experimental Procedures") revealed nearly maximal activation by 3.2 μM ADPR in the presence of 200 μM AMP (Fig. 3*D*, *gray bar*; compare with *white bar*) and a lack of current increase following AMP removal (Fig. 3*D*, *black bar*).

Finally, to examine whether a possible inhibitory effect of AMP might be masked by the facilitatory effect of our saturating $[Ca^{2+}]_i$, we repeated experiments similar to those shown in Fig. 3 (*C* and *D*) at a suboptimal $[Ca^{2+}]_i$ of 15 μM (Fig. 3, *E* and *F*). However, just as in the presence of saturating Ca^{2+}, pre-exposure to 200 μM AMP in 15 μM $[Ca^{2+}]_i$ again failed to affect fractional activation by subsequently added 3.2 μM ADPR (Fig. 3*E*; Fig. 3*F*, *gray bar*, compare with Fig. 1*B* and *white symbols* in Fig. 1*C*), and no further current increase was observed upon AMP removal (Fig. 3, *E* and *F*, *black bar*). These results suggest that AMP-mediated inhibition of TRPM2 whole-cell currents is not a direct effect of AMP on the TRPM2 protein.

Effects of Commercial cADPR on TRPM2 Currents in Cell-free Patches—Given the large scatter in the potency of cADPR to activate TRPM2 currents in intact cells of various sources (4, 5, 16–18), we tested whether direct superfusion of inside-out patches with a solution containing 10 μM cADPR and saturating Ca^{2+} would elicit any TRPM2 currents. To our surprise, 10 μM cADPR maximally stimulated TRPM2 channels in patches, as witnessed by a lack of further current increase upon the addition of a saturating dose (10 μM) of ADPR (Fig. 4*A*). As little as 1 μM cADPR elicited sizeable TRPM2 currents; a dose-response curve of fractional activation by cADPR yielded a $K_{1/2}$ of 1.6 ± 0.3 μM (Fig. 4*B*), only ~2-fold larger than the $K_{1/2}$ for ADPR measured under identical conditions (Fig. 1, *A* and *C*). We next examined whether a synergy between submaximal concentrations of cADPR and ADPR, as observed in intact cells (16–18), could be reproduced in a cell-free system by first applying 1 μM cADPR in saturating Ca^{2+} and then adding increasing concentrations of ADPR to this background (Fig. 4*C*). At this concentration cADPR alone elicited ~30% of maximal activity, which was further increased in a dose-dependent manner by subsequently applied ADPR. The dose-response curve for activation by ADPR in the presence of a fixed concentration of 1 μM cADPR (Fig. 4*D*, *black symbols*) was fitted to a modified Hill equation to yield a $K_{1/2}$ of 0.8 ± 0.1 μM for ADPR. Thus, the presence of a submaximal concentration (1 μM) of cADPR did not significantly affect the apparent affinity for ADPR activation (Fig. 1, *A* and *C*). The high affinity potent stimulation by cADPR alone, together with the lack of synergy with ADPR, raised the possibility of a substantial contamination of our cADPR stock by ADPR, as had been observed in another study (5). Indeed, mass spectrometric analysis (not shown) of an aliquot of cADPR from the same batch revealed an estimated ~50% of contaminant ADPR, which, on its own, could account for the apparent affinity observed for stimulation by our cADPR solutions (Fig. 4*B*).

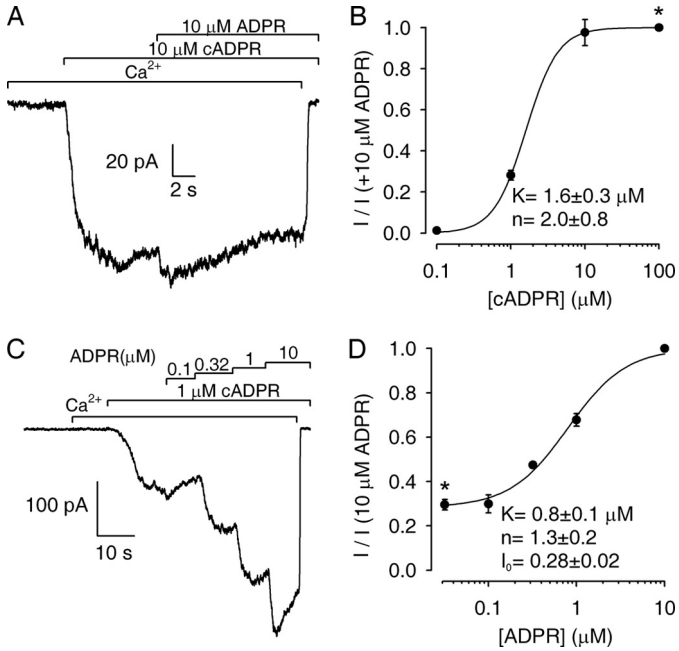

FIGURE 4. **Effects of commercial cADPR on TRPM2 currents.** *A*, exposure of an inside-out patch to 10 μM commercial cADPR, in the presence of saturating (125 μM) Ca^{2+}, activates a large TRPM2 current, which is little enhanced by the addition of 10 μM ADPR (*bars*). *B*, dose-response curve for fractional activation by commercial cADPR. Currents activated by 0.1, 1, and 10 μM commercial cADPR were normalized to that obtained in the same patch by subsequent addition of saturating (10 μM) ADPR. The *rightmost symbol* (marked by *) illustrates the maximal current in the presence of 10 μM ADPR and corresponds to an open probability close to unity (9). The *solid line* is a fit to the Hill equation; fit parameters are indicated in the panel. *C*, TRPM2 currents are activated by 1 μM commercial cADPR in the presence of saturating Ca^{2+}, followed by the addition of increasing concentrations of ADPR. *D*, fractional activation by ADPR in the presence of 1 μM commercial cADPR. The currents were normalized to that obtained in the presence of 10 μM ADPR in the same patch. The *leftmost symbol* (marked by *) denotes fractional current activated by 1 μM commercial cADPR on its own. The *solid line* is a fit to a modified Hill equation of the form $I([ADPR]) = I_o + (I_\infty - I_o)*([ADPR]^n/(K^n + [ADPR]^n))$; fit parameters are indicated in the panel.

Refined Purification Procedure Yields Functionally Pure cADPR—To obtain a cADPR solution devoid of contaminating ADPR, cADPR stock solution was treated with nucleotide pyrophosphatase (P7383; Sigma), which degrades ADPR (but not cADPR) into AMP plus ribose-5-phosphate, followed by removal of the enzyme by filtering (5). To minimize potential artifacts, we verified three aspects of this procedure.

First, the efficiency of the enzymatic digestion was monitored by TLC (Fig. 5*A*; see "Experimental Procedures"). Loading a sample of untreated cADPR onto the TLC plate resulted in two distinct spots, the faster one co-migrating with ADPR and accounting for ~20% of total density in this batch (Fig. 5*A*, compare two *right lanes*). In contrast, in a sample of enzymatically treated cADPR, the spot corresponding to ADPR was absent, replaced by a slow spot of comparable density co-migrating with AMP (Fig. 5*A*, compare two *left lanes*), confirming enzymatic conversion of contaminant ADPR into AMP and ribose-5-phosphate. (Ribose-5-phosphate elicits no fluorescence and is therefore not visible on the TLC.)

Second, our enzymatically purified cADPR solution contains AMP and ribose-5-phosphate (~2–5 μM each for 10 μM

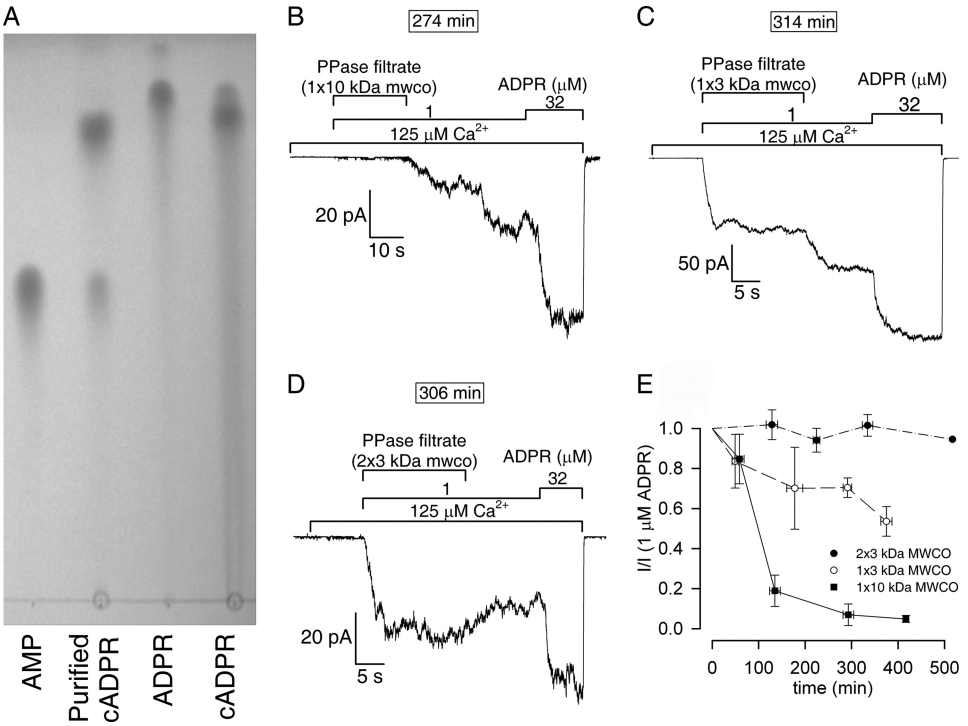

FIGURE 5. **Testing of the cADPR purification procedure.** *A*, TLC analysis of (from *left* to *right*) AMP, enzymatically purified cADPR, ADPR, and nontreated cADPR. For all samples 20 nmol of nucleotide were loaded, followed by drying. Note conversion of the ADPR contamination of nontreated cADPR into AMP in the enzymatically purified cADPR sample. *B–D*, activation of TRPM2 currents by 1 μM ADPR solutions containing an aliquot of nucleotide pyrophosphatase filtrate and by pure 1 μM ADPR (*bars*). 10- and 3-kDa molecular mass cut-off filter columns were used to produce the filtrates for the experiments in *B* and *C*, respectively. For the experiment in *D*, the filtrate was produced by sequential passages through two 3-kDa molecular mass cut-off filter columns. Approximate timing of the start of each experiment relative to addition of the filtrate to the test solution is indicated *above* each panel. *E*, fractional current activated by test solutions containing 1 μM ADPR + nucleotide pyrophosphatase filtrate, normalized to the current supported by 1 μM ADPR in the same patch, as a function of time following the addition of the filtrate to the test solution. The *symbols* with *error bars* represent the values averaged over 2–10 experiments with similar timing. The three time courses represent three protocols for producing the filtrate (*panels B–D*): 1× passage through 10-kDa molecular mass cut-off filter (*black squares*), 1× passage through 3-kDa molecular mass cut-off filter (*white circles*), and 2× passage through 3-kDa molecular mass cut-off filters (*black circles*).

cADPR). We therefore tested whether these two breakdown products could affect TRPM2 channel activity. However, in control experiments application of AMP (100 μM) or ribose-5-phosphate (100 μM) alone or co-application of 100 μM AMP + 100 μM ribose-5-phosphate did not affect TRPM2 current activation by 1 or 32 μM ADPR in saturating Ca^{2+}.

Third, although a filter with a 10-kDa molecular mass cut-off, as described in Ref. 5, seems adequate for removal of the 24-kDa nucleotide pyrophosphatase, we wanted to functionally verify the efficacy of this crucial step. This is because in experiments in which purified cADPR is co-applied with ADPR, any residual enzymatic activity might result in slow degradation of ADPR, yielding decreased channel activity. Because TRPM2 activity is most sensitive to [ADPR] in a concentration range near ~1 μM, fractional TRPM2 current in nominally 1 μM ADPR is a sensitive measure of any remaining ADPRase activity. We therefore filtered an aliquot of nucleotide pyrophosphatase equivalent to that used for treatment of one batch of cADPR through a 10-kDa molecular mass cut-off filter column. An aliquot of this filtrate equivalent to that used for obtaining a final concentration of 10 μM purified cADPR was added to a bath solution containing 1 μM ADPR. Fractional TRPM2 current activation by this test solution, relative to that obtained with 1 μM untreated ADPR, was assayed in excised patches at various times (0–7 h) following the addition of the filtrate to the test solution. To our surprise, the ability of the test solution to activate TRPM2 channels was virtually abolished within 2–3 h of the addition of the filtrate; Fig. 5*B* shows a current trace from a patch obtained ~4 h after the test solution had been prepared. The time-dependent decline of fractional TRPM2 activity supported by this test solution (Fig. 5*E*, *black squares*) is a measure of the rate at which ADPR is slowly degraded by residual pyrophosphatase activity in the filtrate. To reduce this enzymatic contamination, we passed a similar aliquot of the pyrophosphatase through a 3-kDa molecular mass cut-off filter column. Adding an equivalent amount of this filtrate to a 1 μM ADPR solution yielded a test solution that still showed a time-dependent decline in its efficiency to activate TRPM2, but the rate of this decline was dramatically reduced (Fig. 5*C*, current trace obtained ~5 h after the addition of the filtrate; and Fig. 5*E*, *white circles*, time course of fractional current activation). Finally, sequential filtering of the pyrophosphatase through two 3-kDa molecular mass cut-off columns resulted in a filtrate that, when added to a 1 μM ADPR solution, did not decrease the efficiency of this solution to activate TRPM2 currents even after incubation times of ~9 h (Fig. 5, *D* and *E*, *black circles*), signaling complete removal of the pyrophosphatase activity by this filtering protocol.

These results establish that treatment of cADPR with the nucleotide pyrophosphatase, followed by 2-fold filtering through 3-kDa molecular mass cut-off filter columns, yields a purified cADPR stock solution devoid of any factors that could distort the effect of cADPR on TRPM2 activity. All of the experiments in the following section in which cADPR and ADPR were co-applied were performed within 3 h of adding purified cADPR to the bath solutions.

Pure cADPR Neither Activates TRPM2 nor Sensitizes TRPM2 to Activation by ADPR in Cell-free Patches—We next tested enzymatically purified cADPR for its ability to activate TRPM2. However, 10 μM purified cADPR applied in the presence of saturating Ca^{2+} elicited no channel activity even in patches in which subsequent application of saturating ADPR could activate hundreds of TRPM2 channels (Fig. 6*A*); fractional currents in 10 μM pure cADPR, normalized to the currents obtained in ADPR in the same patch, averaged 0.012 ± 0.003 (n = 23) (Fig. 6*C*, *leftmost bar*). We also verified whether pure cADPR could

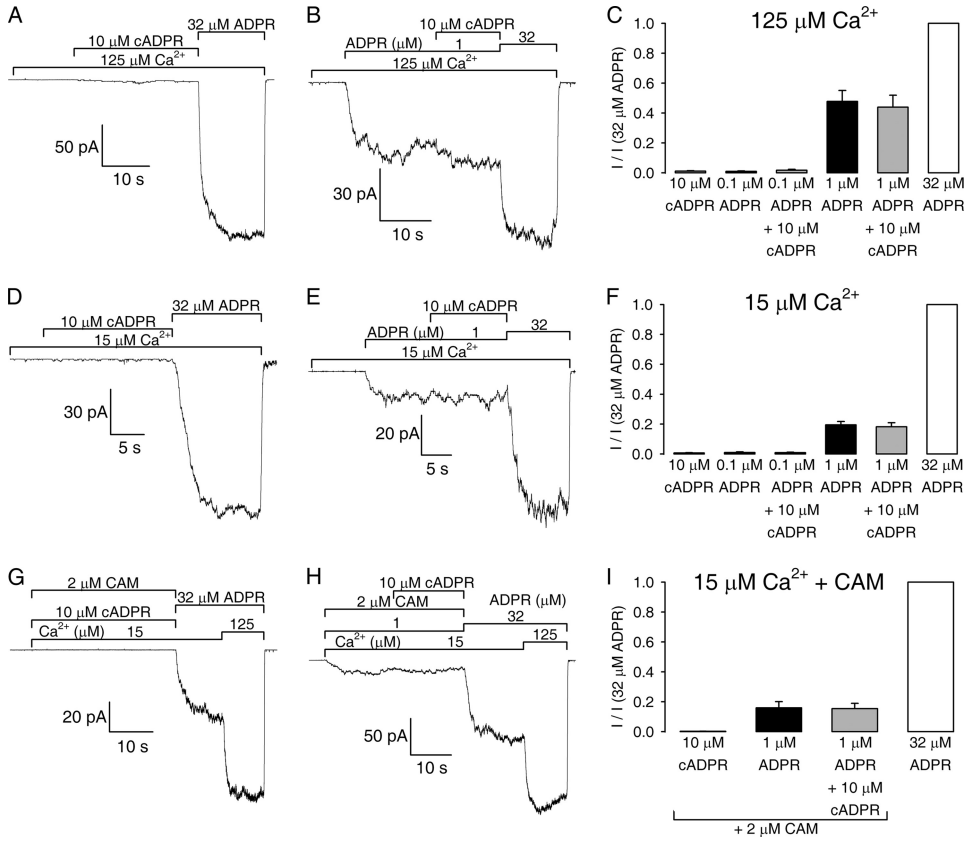

FIGURE 6. **Pure cADPR does not stimulate TRPM2 channel activity in cell-free patches.** *A*, *D*, and *G*, no currents are activated by direct superfusion of inside-out patches with 10 μM purified cADPR in the presence of 125 μM Ca^{2+} (*A*), 15 μM Ca^{2+} (*D*), or 15 μM Ca^{2+} + 2 μM calmodulin (*CAM*) (*G*), whereas subsequent exposure to 32 μM ADPR elicits large currents in all three cases. *B*, *E*, and *H*, co-application of 10 μM purified cADPR does not enhance fractional TRPM2 currents activated by 1 μM ADPR in the presence of 125 μM Ca^{2+} (*B*), 15 μM Ca^{2+} (*E*), or 15 μM Ca^{2+} + 2 μM calmodulin (*H*). *C*, *F*, and *I*, fractional currents activated by 10 μM purified cADPR (*leftmost bars*) and by 0.1 or 1 μM ADPR in the absence (*black bars*) and presence (*gray bars*) of 10 μM purified cADPR; the three panels illustrate the results obtained in the presence of 125 μM Ca^{2+} (*C*), 15 μM Ca^{2+} (*F*), or 15 μM Ca^{2+} + 2 μM calmodulin (*I*), respectively. The currents were normalized to those elicited in the same patch by 32 μM ADPR (*white bars*). The *error bars* represent S.E. Correction for rundown was done as described for supplemental Fig. S1.

enhance currents activated by a subthreshold concentration of 0.1 μM or by a half-saturating concentration of 1 μM, ADPR (Fig. 6*B*). However, the currents elicited by these submaximal concentrations of ADPR were not affected by the addition of 10 μM purified cADPR (Fig. 6*C*, *black* and *gray bars*). This lack of a potentiating effect of purified cADPR was not due to our use of saturating $[Ca^{2+}]_i$, because even at a subsaturating (15 μM) $[Ca^{2+}]_i$, 10 μM purified cADPR failed to activate TRPM2 currents when applied on its own (Fig. 6, *D* and *F*, *leftmost bar*) and failed to affect TRPM2 currents elicited by 0.1 or 1 μM ADPR (Fig. 6, *E* and *F*, *black* and *gray bars*).

In principle, the lack of effect of cADPR on TRPM2 activity in excised patches might be due to the loss of some cellular factor required for a direct action of cADPR on TRPM2. Because calmodulin has been implicated in the regulation of TRPM2 activity (13, 27), we tested whether the whole-cell effects of cADPR could be reproduced in a cell-free system continuously supplied with calmodulin. However, even in the presence of 2 μM calmodulin (and subsaturating Ca^{2+}), purified cADPR (10 μM) failed to elicit TRPM2 currents (Fig. 6, *G* and *I*, *leftmost bar*) or to enhance TRPM2 activity in 1 μM ADPR (Fig. 6, *H* and *I*, *black* and *gray bars*).

In Cell-free Patches NAADP Is a Low Affinity Partial Agonist and Does Not Sensitize TRPM2 to Activation by ADPR—The recently identified stimulation of TRPM2 activity by the Ca^{2+} mobilizing second messenger NAADP, both on its own and in synergy with ADPR, prompted us to test the effect of this nucleotide in our cell-free system. Although in the presence of saturating Ca^{2+} ADPR activates TRPM2 currents with a $K_{½}$ of ~1 μM (Fig. 1, *A* and *C*), for NAADP we had to apply concentrations in the tens of micromolar range to elicit any currents (Fig. 7*A*). Moreover, even at a saturating concentration (1 mM), NAADP could only partially stimulate TRPM2 activity, as reflected by an approximate doubling of the current by subsequently applied 32 μM ADPR (Fig. 7*A*). The dose-response curve for fractional current activation by NAADP (Fig. 7*E*, *black squares*) identifies this compound as a low affinity partial agonist; a fit to the Hill equation yielded $K_{½}$ = 104 ± 16 μM and a maximal fractional current of 0.49 ± 0.04 relative to that obtained in saturating ADPR in the same patch. This effect of NAADP seems safely attributable to the compound itself, because TLC analysis of our NAADP sample did not reveal any detectable contamination by ADPR (Fig. 7*F*).

We also examined a possible synergy by submaximal concentrations of NAADP and ADPR. To test whether NAADP could enhance the sensitivity for ADPR activation, we first exposed TRPM2 channels to 50 μM NAADP followed by stepwise addition of increasing concentrations of ADPR (Fig. 7*B*). However, the midpoint of the resulting dose-response curve (Fig. 7*E*, *white circles*) was not different from that obtained for ADPR alone (Fig. 7*E*, *black circles*, replotted from Fig. 1*C*); fitted $K_{½}$ for ADPR activation in the presence of 50 μM NAADP was 1.2 ± 0.1 μM. Conversely, stepwise activation of TRPM2 currents by increasing concentrations of NAADP, all in the presence of 0.1 μM ADPR (Fig. 7*C*), yielded a dose-response curve (Fig. 7*E*, *white squares*) that was only slightly shifted (fitted $K_{½}$ = 48 ± 10 μM) relative to the one obtained in the absence of ADPR (Fig. 7*E*, *black squares*).

Because a potential NAADP effect could be masked at our saturating $[Ca^{2+}]_i$, we also measured fractional current activation (relative to that obtained in 32 μM ADPR in the same patch) by 50 μM and 1 mM NAADP, all in the presence of subsaturating $[Ca^{2+}]_i$ (15 μM). However, this lowered $[Ca^{2+}]_i$ did not increase the apparent affinity for activation by NAADP,

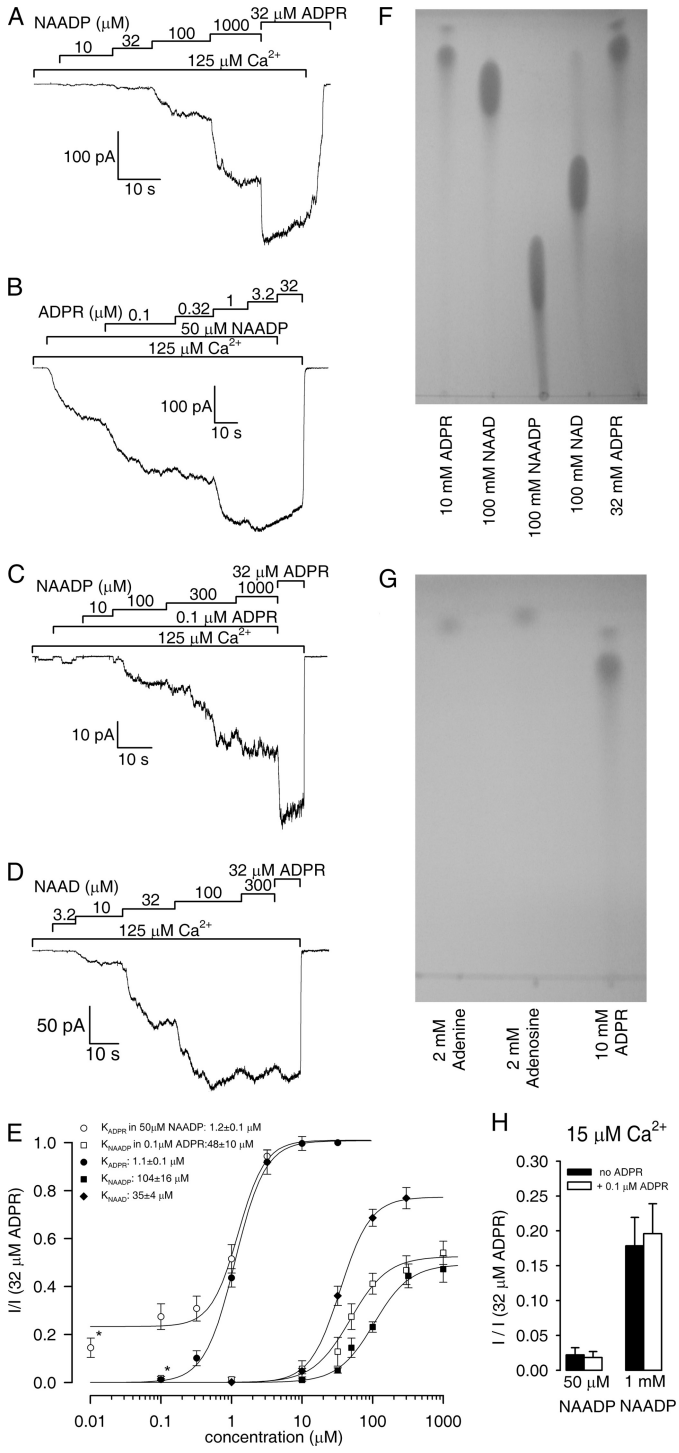

FIGURE 7. **NAADP and NAAD are low affinity direct activators of TRPM2.** *A–D*, TRPM2 currents are activated in inside-out patches by superfusion with increasing concentrations of NAADP (*A* and *C*), ADPR (*B*), or NAAD (*D*) in the presence of saturating Ca^{2+} (*bars*). In *B* and *C*, 50 μM NAADP and 0.1 μM ADPR, respectively, were applied throughout the exposure to the tested nucleotide (*bars*). *E*, dose-response curves for fractional activation by NAADP (*black squares*), NAAD (*black diamonds*), ADPR (*black circles*, replotted from Fig. 1*C*), ADPR in the presence of a constant 50 μM NAADP (*white circles*), and NAADP in the presence of a constant 0.1 μM ADPR (*white squares*); the *leftmost* data points for the latter two curves (*) represent zero agonist concentrations. All of the curves were obtained in the presence of saturating Ca^{2+} and normalized to the current obtained in 32 μM ADPR in the same patch; the latter corresponds to an open probability of close to unity (9). The *solid lines* represent fits to the Hill equation; the predicted midpoints are printed in the panel. For the fit to the ADPR dose-response curve in the presence of 50 μM NAADP, a constant term was included (see Fig. 4*D*). *F*, TLC analysis of 1-μl aliquots of (from *left* to *right*) 10 mM ADPR, 100 mM NAAD, 100 mM NAADP, 100 mM NAD, and 32 mM ADPR. Note ADPR contamination in NAD, and a rapidly migrating contaminant in ADPR (also visible in Fig. 5*A*). *G*, TLC analysis of 1-μl aliquots of (from left to right) 2 mM adenine, 2 mM adenosine, and 10 mM ADPR. The rapidly migrating contaminant in ADPR is fluorescent and roughly co-migrates with adenine. *H*, fractional activation by 50 μM (*left*) and 1 mM (*right*) NAADP in the absence (*black bars*) and presence (*white bars*) of 0.1 μM ADPR at subsaturating (15 μM) $[Ca^{2+}]_i$; the currents were normalized to that obtained in the same patch in the presence of 15 μM Ca^{2+} + 32 μM ADPR. Correction for rundown was done as described in supplemental Fig. S1. The *error bars* in *E* and *H* represent S.E.

because 50 μM NAADP again elicited only ~10% of the current obtained with 1 mM NAADP (Fig. 7*H*, *black bars*; compare with Fig. 7*A* and *black squares* in Fig. 7*E*). Moreover, the efficacy of NAADP actually seemed to decrease at this lower $[Ca^{2+}]_i$, because the maximal current evoked by 1 mM NAADP was only ~20% of that supported by 32 μM ADPR (Fig. 7*H*, *right black bar*). Finally, even at 15 μM $[Ca^{2+}]_i$, the presence of 0.1 μM ADPR did not affect fractional current activation by 50 μM and 1 mM NAADP (Fig. 7*H*, *white versus black bars*). Thus, the low affinity and low efficacy of NAADP activation (Fig. 7, *A* and *E*) and the lack of synergy between NAADP and ADPR (Fig. 7, *B*, *C*, and *E*) in inside-out patches are not attributable to our use of a saturating $[Ca^{2+}]_i$.

NAAD Is a Low Affinity Direct Activator of TRPM2 Channels—NAAD, the dephospho-form of NAADP, has not yet been tested for its ability to modulate TRPM2 currents. Because NAAD is structurally more similar to ADPR than NAADP, we extended our study to include this nucleotide. NAAD resembled NAADP in that it could stimulate TRPM2 currents at high concentrations but seemed more efficient than NAADP in opening the channels at saturating concentrations, because subsequent application of 32 μM ADPR caused little further current enhancement (Fig. 7*D*). Fitting the NAAD dose-response curve (Fig. 7*E*, *black diamonds*) yielded $K_{1/2} = 35 \pm 4$ μM and a maximal fractional current of 0.77 ± 0.04. Based on these fit parameters and the lack of detectable ADPR contamination in our NAAD stock (Fig. 7*F*), this compound can be classified as a low affinity full agonist of TRPM2. In contrast, we could not address the controversial activation of TRPM2 by NAD (3, 4, 16, 19), because TLC analysis revealed a substantial contamination of our NAD stock solution by ADPR (Fig. 7*F*).

DISCUSSION

Since the initial identification of ADPR and Ca^{2+} as the primary agonists of TRPM2 (2, 3), a cation channel that becomes activated in cells subjected to oxidative stress (4), several studies have undertaken to elucidate the connection between reactive oxygen species- and ADPR-mediated TRPM2 activation (4, 14, 15). At the same time, the search for potential additional TRPM2 modulators has identified several adenine nucleotides as potential candidates for affecting TRPM2 gating, including cADPR, AMP, NAADP, and *O*-acetylated ADPR (4, 5, 16–19). However, many of the described effects, particularly those of H_2O_2 and cADPR, have remained controversial, and the reported apparent affinities for all of the above compounds scatter over several orders of magnitude. The most likely reason for these discrepancies is that all of the above studies have been

conducted in intact cells with limited control over the intracellular concentrations of metabolites, which are rapidly formed, degraded, and/or compartmentalized by an intact cellular machinery. For the same reason, these studies have not allowed any conclusions regarding whether the newly identified modulators act directly, by binding to the TRPM2 protein, or indirectly, by altering the local concentrations of the primary agonists in the vicinity of the channels. Further uncertainty was provided by reported impurities in commercially available nucleotide preparations (5, 19). In the present study we have examined for the first time the effects of the above compounds in cell-free inside-out patches of membrane, which allowed us to identify direct effectors of TRPM2 channel activity.

Direct superfusion of the cytosolic face of the TRPM2 protein by a large concentration (1 mM) of H_2O_2 for periods up to 60 s did not result in channel activation (Fig. 2, *A*, *left panel*, and *B*), precluding the possibility that H_2O_2-induced activation of TRPM2 currents might reflect oxidation of some residues on the cytosolic surface of the channel. Because H_2O_2 exposure also failed to inhibit maximal TRPM2 currents induced by saturating ADPR (Fig. 2*A*, *right panel*, and *B*) and did not affect the apparent affinity for ADPR (Fig. 2*B*), we conclude that any potential oxidation of TRPM2 residues by H_2O_2 is unlikely to have a functional consequence. These results are congruent with previous interpretations that oxidative stress leads to TRPM2 activation in cells by promoting accumulation of free ADPR (15) and/or Ca^{2+} in the vicinity of the channels (also see Ref. 4) and suggest that the recently described synergism between subthreshold concentrations of H_2O_2 and ADPR for activation of TRPM2 whole-cell currents (16, 17) is not due to a direct effect of H_2O_2 on the TRPM2 channel.

In our cell-free system we did not observe inhibition of ADPR-induced TRPM2 currents by AMP, reported to occur in intact cells with IC_{50} values between 10 and 70 μM (16, 17), even when AMP was applied at a 60-fold excess relative to ADPR (Fig. 3). This finding is in contrast with TRPM4 channels (28) and TRPM4-like cation channels in brain endothelium (30), which are inhibited with high affinity by AMP in inside-out patches. Thus, although both the C-terminal NUDT9-H domain and the N-terminal TRPM homology region seemed to be potential candidates for binding inhibitory AMP, in the case of TRPM2 the AMP effect must be indirect. In intact cells AMP is a strong metabolic signal that regulates cellular energy production through several signaling pathways including AMP kinase (reviewed in Ref. 31). Therefore, intracellular dialysis of large concentrations of AMP likely causes drastic changes in cellular metabolism that are expected to be cell type-specific. Elucidating how these changes ultimately result in TRPM2 inhibition will be a target of future investigations.

Activation of TRPM2 current by commercial cADPR (Fig. 4) was entirely due to heavy contamination of our cADPR preparation by ADPR (Fig. 5*A*, *right lane*), because enzymatic removal of ADPR abolished activation of TRPM2 by cADPR (Fig. 6*A*). Further, we could observe no sign of sensitization toward ADPR stimulation by 10 μM pure cADPR in our cell-free system (Fig. 6, *B* and *C*), in contrast to a reported 100-fold lowering of $K_{1/2}$ for ADPR by dialysis of 10 μM cADPR into cells (16). A result similar to ours, obtained with enzymatically treated cADPR in intact cells (5), was argued to reflect clouding of the stimulatory cADPR effect by inhibitory AMP, which is produced by the nucleotide pyrophosphatase treatment (17). In the present experiments such an antagonizing effect can be excluded, because in our cell-free system AMP had no effect on TRPM2 activity even at a concentration of 200 μM (Fig. 3, *B–F*), whereas our test solutions with 10 μM purified cADPR contained only an estimated 2–5 μM AMP (Fig. 5*A*). Similarly, ribose-5-phosphate, the other breakdown product present in our purified cADPR solution, neither stimulated nor inhibited TRPM2 activity even at a concentration of 100 μM (2, 16), whether applied alone or in combination with AMP. Thus, we conclude that cADPR, at least at concentrations up to 10 μM, does not directly stimulate or potentiate stimulation of TRPM2 activity. Taking into account that resting intracellular ADPR concentrations are low micromolar (5), whereas cADPR concentrations were found to be in the nanomolar range (*e.g.* ~200 nM in brain (32), ~50 nM in HL-60 leukemia cells (32), ~500 nM in Jurkat T-cells (33), and ~200 nM in neutrophil granulocytes (5)) and remained <2 μM following cell stimulation by various activating signals (5, 32, 33), any possible direct effects on TRPM2 of cADPR concentrations higher than 10 μM would hardly have physiological relevance. One possible explanation for the observed apparent synergism between low concentrations of cADPR and ADPR in cells (16–18) might be mobilization of Ca^{2+} by cADPR acting on ryanodine receptors (24). Although in one study that reported ADPR-cADPR synergism bulk intracellular [Ca^{2+}] was not elevated by cADPR dialysis, elevation of [Ca^{2+}] in microdomains in the vicinity of TRPM2 could not be excluded (16).

Consistent with whole-cell reports (17, 18), we confirm low affinity activation of TRPM2 by NAADP in inside-out patches (Fig. 7*A*). Because by TLC we could not detect any significant ADPR contamination in our NAADP stock (Fig. 7*F*), we conclude that this activating effect is a consequence of direct binding of NAADP to TRPM2. However, a direct comparison of TRPM2 currents activated by saturating concentrations of NAADP and ADPR in the same patch revealed only ~50% activation by NAADP, identifying the latter as a partial agonist (Fig. 7, *A* and *E*). Given the 100-fold lower apparent affinity for NAADP ($K_{1/2}$ = ~100 μM; Fig. 7*E*) (17, 18) as compared with ADPR and the low nanomolar concentrations of this nucleotide in living cells (~60 nM in red blood cells (34), ~20 nM in hepatocytes, (34), ~4 nM in resting, and ~30 nM in stimulated Jurkat T-cells (24)), this partial agonist mechanism cannot be considered physiologically relevant. On the other hand, the more promising strong synergism between low concentrations of NAADP and ADPR observed in living cells (*i.e.* full activation by a combination of subthreshold concentrations of ADPR and NAADP (18)) is not observed in a cell-free system (Fig. 7, *B*, *C*, and *E*) and must therefore reflect some indirect effect of NAADP in intact cells, such as an influence on local [Ca^{2+}] and/or on local [ADPR] in the vicinity of TRPM2.

Because our results suggested that NAADP can bind, albeit with low affinity, to the ADPR-binding site on TRPM2, we reasoned that the dephosphorylated form NAAD might be a better agonist given its closer structural resemblance to ADPR. Our data indeed confirmed that removal of the phosphate group

from NAADP increases the apparent affinity by ~3-fold and also enhances the efficacy for channel opening (Fig. 7, *D* and *E*).

Whether NAD is a true activator of TRPM2 is still an open question. Early studies suggested NAD as the primary activator of TRPM2 (3, 4), but the very low affinity of this activation ($K_{½} > 1$ mM (4, 16)), together with demonstrated significant contamination of commercial NAD preparations by ADPR (16, 19), has cast doubt on this original interpretation. Our demonstration of a low affinity direct activation of TRPM2 by NAAD ($K_{½} = 35$ μM), together with the structural resemblance of this nucleotide to NAD, raises the possibility that NAD might also act as a low affinity direct agonist of TRPM2, and this might even bear physiological relevance given the high cytosolic NAD concentrations in living cells (4). Unfortunately, the substantial contamination of commercially available NAD by ADPR, also confirmed by our TLC analysis (Fig. 7*F*), prevents us from addressing this question. An important corollary of our studies is that the purity of nucleotide preparations must be seriously considered when studying TRPM2 regulation. Indeed, even in our stock of ADPR, our TLC studies detected a small (~10%) contamination by a hydrophobic compound that runs almost at the solution front (Figs. 5*A* and 7, *F* and *G*), roughly co-migrating with adenine (Fig. 7*G*; note that unlike ribose-5-phosphate, the contaminant in ADPR is fluorescent, suggesting the presence of the adenine base). In control experiments (not shown) adenosine and adenine neither activated nor inhibited TRPM2 currents at concentrations of 10 μM, ~3-fold higher than we would expect them to be present in our saturating 32 μM ADPR solution.

Because we were unable to reproduce in our cell-free system several of the effects reported in intact cells for the compounds under study, we wondered whether this discrepancy might be attributable to some specific environmental parameter in our experiments. Along these lines, we considered the possibility that the reported stimulation by H_2O_2 (4, 14, 16) and cADPR (17, 18), inhibition by AMP (16, 17), or sensitization toward ADPR activation by H_2O_2 (16, 18), cADPR (16–18), and NAADP (18) might require these compounds to bind to the same site(s) to which activating Ca^{2+} binds (in this case saturation by Ca^{2+} might make these sites unavailable for binding the agonist/antagonist of interest) or that they might share a common stimulatory mechanism. In both cases the modulatory effect of the agonist of interest could be masked at our saturating $[Ca^{2+}]_i$. Although even in intact cells open channels likely experience saturating, high micromolar, local $[Ca^{2+}]_i$ (9, 26), we extended our studies to a $[Ca^{2+}]_i$ of 15 μM, which is lower than the $K_{½}$ for Ca^{2+} activation (~20 μM) (9) and is expected to leave more than half of the Ca^{2+}-binding sites free at any time. However, even at this suboptimal $[Ca^{2+}]_i$, which resulted in a moderate shift in the dose-response curve for ADPR activation (Fig. 1, *B* and *C*), we could not detect any activation by H_2O_2 (Fig. 2, *C* and *D*), any inhibition by AMP (Fig. 3, *E* and *F*), or any synergistic effects when co-applying H_2O_2 + ADPR (Fig. 2, *C* and *D*), cADPR + ADPR (Fig. 6, *E* and *F*), or NAADP + ADPR (Fig. 7*H*). Thus, the reported whole-cell effects of H_2O_2, AMP, cADPR, and NAADP do not involve binding of these compounds to the activating Ca^{2+}-binding sites on the TRPM2 protein and are mechanistically distinct from the activating effect of Ca^{2+}.

We also considered the possibility that the use of different intracellular cations might be responsible for the discrepancies between our data and various whole-cell studies; to minimize cell type-specific endogenous currents, the physiological intracellular K^+ ion used in some of those studies (16–18) was replaced by Cs^+ in others (4, 14, 18) and Na^+ in the present study. For instance, voltage-dependent inactivation of TRPM2 whole-cell currents was observed in HEK-293 cells loaded with Na^+ (2), and in the same cell line cADPR activated significant whole-cell currents only when intracellular K^+ was replaced by Cs^+ (18), although the latter phenomenon was attributed to some indirect effect of Cs^+ on ADPR metabolism. Even though in an earlier study we have shown that in inside-out patches intracellular Na^+ does not confer voltage dependence to TRPM2 gating and that the apparent affinities of ADPR and Ca^{2+} for activating TRPM2 are the same using intracellular Na^+ or K^+ (9), in that study ADPR activation was studied only at saturating $[Ca^{2+}]_i$, and synergism between potential co-activators was not addressed. We therefore also investigated the dose dependence for ADPR activation in inside-out patches using a K^+-gluconate based bath solution and a subsaturating (15 μM) Ca^{2+} concentration. However, this dose-response relationship (supplemental Fig. S2*A*) was again identical to that obtained in symmetrical Na^+ solution (Fig. 1*C*, *white symbols*). Moreover, substituting K^+ for intracellular Na^+ affected neither the potency nor the efficacy of NAADP to activate TRPM2 currents in subsaturating (15 μM) Ca^{2+}; as reflected by fractional currents evoked by 50 μM and 1 mM NAADP (supplemental Fig. S2*B*, *black bars*), which remained identical to those measured using Na^+ (Fig. 7*H*, *black bars*). Finally, even in a K^+-based bath solution and subsaturating Ca^{2+}, we could detect no sign of synergism when co-applying low concentrations of NAADP and ADPR (supplemental Fig. S2B, *white bars*). Thus, neither intracellular Na^+ nor saturating Ca^{2+} used in most of our experiments are responsible for the absence in a cell-free system of the modulatory effects observed in intact cells. Taken together, the most likely explanation is that those whole-cell effects are indirect, although it remains a formal possibility that H_2O_2, AMP, cADPR, or NAADP might bind directly to the TRPM2 protein but require the presence of a factor, lost during patch excision, to exert their effects on TRPM2 activity. We have ruled out the possibility that the loss of calmodulin in excised patches might be the culprit for the observed low Ca^{2+} affinity (Fig. 1, *D–F*) or the lack of effect of cADPR (Fig. 6, *G–I*) but cannot exclude the role of some other, as yet unidentified, cellular factor.

In conclusion, we have shown that in inside-out patches H_2O_2, AMP, and pure cADPR do not directly affect TRPM2 channel activity, whereas NAADP is a low affinity partial agonist but does not directly potentiate ADPR-mediated activation. Finally, we have also identified NAAD as a low affinity full agonist. Our work suggests that the local concentrations of the primary ligands, ADPR and Ca^{2+}, should be regarded as a final common pathway through which other signaling molecules can indirectly modulate TRPM2 channel activity in living cells.

Acknowledgments—We thank Dr. Dorottya Mayer for oocyte isolation and injection, Dr. Attila Ambrus for SDS-PAGE analysis of the nucleotide pyrophosphatase, and Dr. Árpád Somogyi for mass spectrometric analysis of our cADPR stock.

REFERENCES

1. Nagamine, K., Kudoh, J., Minoshima, S., Kawasaki, K., Asakawa, S., Ito, F., and Shimizu, N. (1998) *Genomics* **54,** 124–131
2. Perraud, A. L., Fleig, A., Dunn, C. A., Bagley, L. A., Launay, P., Schmitz, C., Stokes, A. J., Zhu, Q., Bessman, M. J., Penner, R., Kinet, J. P., and Scharenberg, A. M. (2001) *Nature* **411,** 595–599
3. Sano, Y., Inamura, K., Miyake, A., Mochizuki, S., Yokoi, H., Matsushime, H., and Furuichi, K. (2001) *Science* **293,** 1327–1330
4. Hara, Y., Wakamori, M., Ishii, M., Maeno, E., Nishida, M., Yoshida, T., Yamada, H., Shimizu, S., Mori, E., Kudoh, J., Shimizu, N., Kurose, H., Okada, Y., Imoto, K., and Mori, Y. (2002) *Mol. Cell* **9,** 163–173
5. Heiner, I., Eisfeld, J., Warnstedt, M., Radukina, N., Jüngling, E., and Lückhoff, A. (2006) *Biochem. J.* **398,** 225–232
6. Yamamoto, S., Shimizu, S., Kiyonaka, S., Takahashi, N., Wajima, T., Hara, Y., Negoro, T., Hiroi, T., Kiuchi, Y., Okada, T., Kaneko, S., Lange, I., Fleig, A., Penner, R., Nishi, M., Takeshima, H., and Mori, Y. (2008) *Nat. Med.* **14,** 738–747
7. Smith, M. A., Herson, P. S., Lee, K., Pinnock, R. D., and Ashford, M. L. (2003) *J. Physiol* **547,** 417–425
8. Kaneko, S., Kawakami, S., Hara, Y., Wakamori, M., Itoh, E., Minami, T., Takada, Y., Kume, T., Katsuki, H., Mori, Y., and Akaike, A. (2006) *J. Pharmacol. Sci.* **101,** 66–76
9. Csanády, L., and Törocsik, B. (2009) *J. Gen. Physiol* **133,** 189–203
10. Maruyama, Y., Ogura, T., Mio, K., Kiyonaka, S., Kato, K., Mori, Y., and Sato, C. (2007) *J. Biol. Chem.* **282,** 36961–36970
11. Perraud, A. L., Shen, B., Dunn, C. A., Rippe, K., Smith, M. K., Bessman, M. J., Stoddard, B. L., and Scharenberg, A. M. (2003) *J. Biol. Chem.* **278,** 1794–1801
12. McHugh, D., Flemming, R., Xu, S. Z., Perraud, A. L., and Beech, D. J. (2003) *J. Biol. Chem.* **278,** 11002–11006
13. Starkus, J., Beck, A., Fleig, A., and Penner, R. (2007) *J. Gen. Physiol.* **130,** 427–440
14. Wehage, E., Eisfeld, J., Heiner, I., Jüngling, E., Zitt, C., and Lückhoff, A. (2002) *J. Biol. Chem.* **277,** 23150–23156
15. Perraud, A. L., Takanishi, C. L., Shen, B., Kang, S., Smith, M. K., Schmitz, C., Knowles, H. M., Ferraris, D., Li, W., Zhang, J., Stoddard, B. L., and Scharenberg, A. M. (2005) *J. Biol. Chem.* **280,** 6138–6148
16. Kolisek, M., Beck, A., Fleig, A., and Penner, R. (2005) *Mol. Cell* **18,** 61–69
17. Lange, I., Penner, R., Fleig, A., and Beck, A. (2008) *Cell Calcium* **44,** 604–615
18. Beck, A., Kolisek, M., Bagley, L. A., Fleig, A., and Penner, R. (2006) *FASEB J.* **20,** 962–964
19. Grubisha, O., Rafty, L. A., Takanishi, C. L., Xu, X., Tong, L., Perraud, A. L., Scharenberg, A. M., and Denu, J. M. (2006) *J. Biol. Chem.* **281,** 14057–14065
20. Malavasi, F., Deaglio, S., Funaro, A., Ferrero, E., Horenstein, A. L., Ortolan, E., Vaisitti, T., and Aydin, S. (2008) *Physiol. Rev.* **88,** 841–886
21. Koch-Nolte, F., Haag, F., Guse, A. H., Lund, F., and Ziegler, M. (2009) *Sci. Signal.* **2,** mr1
22. Du, J., Xie, J., and Yue, L. (2009) *Proc. Natl. Acad. Sci. U.S.A.* **106,** 7239–7244
23. Ziegler, M. (2000) *Eur. J. Biochem.* **267,** 1550–1564
24. Fliegert, R., Gasser, A., and Guse, A. H. (2007) *Biochem. Soc. Trans.* **35,** 109–114
25. Higashida, H., Yokoyama, S., Hashii, M., Taketo, M., Higashida, M., Takayasu, T., Ohshima, T., Takasawa, S., Okamoto, H., and Noda, M. (1997) *J. Biol. Chem.* **272,** 31272–31277
26. Brasen, J. C., Olsen, L. F., and Hallett, M. B. (2010) *Cell Calcium* **47,** 339–349
27. Tong, Q., Zhang, W., Conrad, K., Mostoller, K., Cheung, J. Y., Peterson, B. Z., and Miller, B. A. (2006) *J. Biol. Chem.* **281,** 9076–9085
28. Nilius, B., Prenen, J., Voets, T., and Droogmans, G. (2004) *Pflugers Arch.* **448,** 70–75
29. Csanády, L., and Adam-Vizi, V. (2004) *J. Gen. Physiol.* **123,** 743–757
30. Csanády, L., and Adam-Vizi, V. (2003) *Biophys. J.* **85,** 313–327
31. Dzeja, P., and Terzic, A. (2009) *Int. J. Mol. Sci.* **10,** 1729–1772
32. Takahashi, K., Kukimoto, I., Tokita, K., Inageda, K., Inoue, S., Kontani, K., Hoshino, S., Nishina, H., Kanaho, Y., and Katada, T. (1995) *FEBS Lett.* **371,** 204–208
33. Guse, A. H., da Silva, C. P., Berg, I., Skapenko, A. L., Weber, K., Heyer, P., Hohenegger, M., Ashamu, G. A., Schulze-Koops, H., Potter, B. V., and Mayr, G. W. (1999) *Nature* **398,** 70–73
34. Churamani, D., Carrey, E. A., Dickinson, G. D., and Patel, S. (2004) *Biochem. J.* **380,** 449–454